Landscape maturity, fold growth sequence and structural style in the Kirkuk Embayment of the Zagros, northern Iraq

Ahmed K. Obaid[1, 2] and Mark B. Allen[1]

[1]Department of Earth Sciences, University of Durham, Durham, UK, DH1 3LE

[2]Department of Geology, College of Science, University of Baghdad, Baghdad, Iraq

a.k.obaid@durham.ac.uk; m.b.allen@durham.ac.uk

Abstract

The Kirkuk Embayment is located in the southwest of the Zagros fold-and-thrust belt of Iraq. Like fold-and-thrust belts worldwide, the Zagros is conventionally understood to have grown sequentially towards the foreland. Here we use landscape maturity analysis to understand anticline growth in the Embayment. Digital Elevation Model (DEM)-based geomorphic indices Hypsometric Integral (HI), Surface Roughness (SR) and their combination Surface Index (SI) have been applied to quantify landscape maturity. The results inform new ideas for the sequence of anticline growth. Maturity indices are highest for the QaraChauq Anticline in the center of the Embayment, then Makhool/Himreen to the south and lastly, the Kirkuk Anticline to the north. The pattern suggests the growth sequence is not classical 'piggy back' thrusting. This result fits the exhumation record, which is loosely constrained by the stratigraphic exposure level. Favored hypotheses for fold growth order are either i) the folds have grown at different times and out of sequence (QaraChauq first, then Makhool/Himreen, and Kirkuk last), or, ii) the growth occurred with different rates of exhumation but at broadly the same time. There are few constraints from available data on syn-tectonic sedimentation patterns. Fold growth across much of the Embayment might have begun within a limited timeframe in the late Miocene–Pliocene, during the deposition of the Mukdadiyah Formation. Another hypothesis is that folds grew in sequence towards the foreland with different rates of exhumation, but we consider this less likely. We also construct a new cross-section for the Embayment, which indicates limited Cenozoic strain: ~5% shortening. Analysis of topography and drainage patterns shows two previously-undescribed anticlines with hydrocarbon trap potential, between the Makhool and QaraChauq anticlines.

Keywords: Kirkuk Embayment, geomorphic indices, Zagros deformation, Surface index.

1. Introduction

The Zagros region is an important area for studies of continental deformation as it forms part of the active Arabia-Eurasia collision zone (Fig. 1). Therefore, approaches using geomorphology, seismicity and geodesy can be used, that are not applicable in ancient and inactive regions of deformation like the Caledonides or the Alps. The Arabia-Eurasia collision is due to the northward movement of the Arabian Plate that resulted in the closure of the Neotethys ocean (Alavi 2007; Blanc et al. 2003; Ghasemi and Talbot 2006; Vera and Gines 2009; McQuarrie 2004). The exact time of initial collision is not well constrained, but most recent estimates put it in the range 25-35 Ma (McQuarrie and van Hinsbergen 2013; Allen and Armstrong 2008). There has been several hundred kilometers of continental convergence after initial collision (Mouthereau et al. 2012), which has been accommodated within an area covering much of southwest Asia, and specifically the territory of Iran, Turkey, Iraq and neighboring countries.

The Kirkuk Embayment (Fig. 2) is of special importance within Zagros as it contains the southwestern limit of deformation in the Zagros fold-and-thrust belt, and a large proportion of the hydrocarbon reserves in Iraq. The region includes the transition between the stable and unstable shelf of the northern part of the Arabian Plate (Jassim and Goff, 2006). It is a key question whether Cenozoic deformation started from the northeast at the continental suture and moved towards the southwest, either in quasi-continuous progression or in a series of pulses (Allen et al. 2013; Farahpour and Hessami 2012; Hessami et al. 2001; Karim et al. 2011; Lawa et al. 2013; Vergés et al. 2011). Koshnaw et al (2017), used patterns of syn-tectonic sedimentation to interpret "out-of-sequence" fold growth, towards the northeast, but as a late, localized exception to a northeast-southwest fold propagation sequence.

Digital elevation models (DEM) and satellite images have proven to be effective datasets for use in morphotectonic studies (Font et al. 2010; Singh and Jain 2009). With the aid of digital data, morphometric indices have therefore been widely used in active tectonic studies (e.g. Alipoor et al. 2011; Andreani et al. 2014; Bagha et al. 2014; Bahrami 2012; Bahrami 2013; Dehbozorgi et al. 2010; Ehsani and Arian 2015; Fard et al. 2015; Keller and Pinter 2002; Mosavi et al. 2015; El Hamdouni et al. 2008). Recently, researchers have used quantitative geomorphic indices maps to assess tectonic activity in many regions in the world. These indices include: surface roughness, hypsometric integral, and surface indices (González et al. 2015; Grohmann

2004; Mahmood and Gloaguen 2012; Shahzad and Gloaguen 2011b; Siddiqui 2014). Such approaches are especially useful where there is a lack of subsurface data and/or difficulty with access, which is the current situation in Iraqi Zagros.

Geomorphic indices are used in this paper to study landscape maturity, with a view to understanding the relative time of fold growth in the Kirkuk Embayment and therefore the sequence of deformation propagation. We also show the capacity of this kind of analysis to identify previously unrecognized folds, which may have hydrocarbon potential.

2. Geological setting and seismotectonics

2.1 Regional tectonics

As a part of the Arabia-Eurasia collision zone, the Zagros belt extends for ~1800 km from south-east Turkey, passing through the north and north-east of Iraq, across southern Iran and ending at the Strait of Hormuz in southeastern Iran (Alavi 2007; Vera and Gines 2009). The Zagros region has been subjected to a series of compressional and extensional phases during its geologic history that have initiated and later reactivated a series of basement faults (Ameen 1992; Jassim and Goff 2006; Stern and Johnson 2010; Burberry 2015). These deformation phases have also led to variations in the facies of the Kirkuk Embayment due to the vertical and horizontal movement of the basement faults (Burberry 2015). GPS data suggests that the region accommodates a northward movement of the Arabian Plate at a rate of ~16 mm/yr. (Vernant et al. 2004) although GPS studies has focused on neighboring territory in Turkey and Iran rather than Iraq itself.

Based on its geomorphology, seismicity, and exposed geology, the Zagros belt has been divided into sub–parallel tectonic units in a number of different ways by different authors. Berberian (1995) used a five–fold division from the northeast to the southwest: the High Zagros Thrust Belt, the Simple Fold Belt, the Zagros Foredeep, the Zagros Coastal Plain, and the Mesopotamian Plain. A simple division is to treat everything southwest of the High Zagros as a part of the Simple Folded Belt, as the boundaries between the lower elevation areas are hard to define consistently along the entire length of the fold-and-thrust belt (Allen et al. 2013).

There are variations in the level of exhumation, relief and surface elevation along the strike of the Zagros from northwest to southeast, which divide the range along tectonic strike into a number of zones, commonly referred to as embayments and salients. The terms are misleading, given that the deformation front of the Zagros is roughly linear in the north where the Kirkuk and Dezful embayments occur, and does not step back from the margins of the intervening Pusht-e Kuh arc (salient). The Fars region forms the remainder of the Zagros to the southeast, and has a curved deformation front, convex to the south (Berberian 1995).

The origins of the two embayments are of interest for hydrocarbon geology in the region, as they contain numerous oil and gas fields in both Kirkuk (Iraq) and Dezful (Iran). These divisions of the Zagros indicate a different distribution of strain along the strike of the range, despite an apparently smooth and continuous convergence pattern of Arabia with Eurasia at the regional scale (McQuarrie et al. 2003; Vernant et al. 2004). Low strains within the embayments are probably complemented in each case by high strain zones to the northeast (McQuarrie 2004; Allen and Talebian 2011); this is consistent with the observed geology of the Bakhtiari Culmination to the north of the Dezful Embayment, but there are not yet equivalent studies in Iraq, north of the Kirkuk Embayment. The Dezful Embayment has been related to the pre-continental collision of the Arabian plate margin, and the irregular distribution of Cretaceous ophiolites upon it (Allen and Talebian 2011). It is not clear that this model applies to the Kirkuk Embayment, however.

The Iraqi sector of the Zagros is commonly mapped as having northeast-southwest trending basement faults (e.g. Jassim and Goff 2006 and references therein). However, it is unclear to what extent these faults are active (Kent 2010; Burberry 2015), or even exist as mapped. As they do not appear to offset the prominent northwest-southeast anticlines that are the focus of this paper, we do not consider them further.

2.2 Stratigraphy

Many formations are exposed in the Kirkuk Embayment (Fig. 3), and many wells have been drilled which help in understanding the depositional environments and ages of geological formations. The Eocene to Pliocene units can be summarized as follows (Bellen et al. 1956; Jassim and Goff 2006), with outcrop photographs in the supplementary file from recent fieldwork near the eastern margin of the Embayment. See also Koshnaw et al. (2017) for a recent description of the Iraqi Zagros stratigraphy.

Avanah Formation (M. Eocene): This unit crops out locally on the southwest flank of the south QaraChauq anticline. It consists primarily of limestone deposited during a highstand.

Kirkuk Group: This unit consists of several formations; Tarjil, Sheikh Alas, and Shurau (Early Oligocene), Baba (Mid. Oligocene), Bajawan, Azkand, and Anah (Late Oligocene). These formations consist of fossiliferous and/or dolomitized, recrystallized limestone.

Euphrates Formation (Early Miocene): This unit is equivalent to part of the Asmari Limestone in Iran. It consists mainly of oolitic to chalky limestone.

Jeribe Formation (Langhian): This formation consists mainly of marly limestone. In many hydrocarbon fields, the whole of the Kirkuk Group, together with the Euphrates and Jeribe formations, represents the main reservoir unit.

Fat`ha Formation (Middle Miocene): The formation is equivalent to the Gachsaran Formation in Iran. It forms the regional topseal for Cenozoic hydrocarbon reservoirs in the Arabia. The lithology is mainly anhydrite, alternating with marl and limestone, with halite northeast of the Kirkuk Embayment (Aqrawi et al. 2010).

Injana Formation (Late Miocene): This unit is the equivalent to the Aghajari (Upper Fars) strata in Iran. South of the Himreen Anticline (the subsidiary type section), the formation consists of 600 m thin-bedded calcareous sandstones, marls, red mudstone, siltstone, and rare fresh water limestone.

Late Miocene Mukdadiyah and Pliocene Bai Hassan formations: The Mukdadiyah Formation is equivalent to the Lower part of the Bakhtiari Formation in Iran (Late Miocene-Early Pliocene). It consists of gavels, sandstones, and red mudstones. The formation reaches its maximum thickness in the Kirkuk Embayment, at ~2000 m. The formation was deposited during anticline growth (Dunnington 1958). This formation is not reported in the northeast of the Zagros, which may mean that it is represented by the Bai Hassan Formation (see below) – with the implication that both the Mukdadiyah and Bai Hassan formations are strongly diachronous.

The Pliocene Bai Hassan Formation (Upper Bakhtiari) consists of sandstone, conglomerate with siltstone and mudstone, and is generally coarser than the Mukdadiyah Formation. The conglomerate layers increase in thickness and frequency towards the northeast.

2.3 Seismotectonics

We have compiled the focal mechanisms available from the instrumental seismicity record (Fig. 2). These data are from the Global CMT catalogue (http://www.globalcmt.org); body-wave modelling studies for the Zagros have not included events from the Iraqi sector of the range (Talebian and Jackson, 2004; Nissen et al., 2011). The earthquake dataset shows that active deformation occurs across the width of the Kirkuk Embayment, similar to the rest of the Zagros, with the caveat that major thrust seismicity is located in the lower elevation portions of the range, below the regional 1250 m elevation contour (Nissen et al. 2011). Kirkuk Embayment earthquakes are a combination of thrusts and strike-slip faults. Thrust earthquake depths, where constrained, are in the upper 20 km of the crust in the rest of the Zagros range to the southeast (Talebian and Jackson 2004). There is a typical uncertainty of 5 km in the depths of events, even where well-constrained. There is no reason to suppose the depth distribution is markedly different for the Iraqi sector of the range, despite the lack of accurate estimates for individual earthquakes. There are two implications of this regional depth distribution. First, seismogenic thrusting is an upper crustal phenomenon, and does not indicate any subduction of the Arabian Plate. Second, crystalline basement must be involved in at least some of the deformation, as the deeper hypocentres are too deep to be nucleated within the sedimentary cover, even allowing for the depth uncertainties noted above.

None of these earthquakes is associated with surface ruptures, so that the identification of the correct nodal plane cannot be done directly. Uncertainties in teleseismically-located epicenters are up to 20 km, making it impractical to link individual events to specific faults in the sub-surface. Either choice of nodal plane in the thrust events is steep (>30°). We assume that northwest-southeast striking plane represents the real fault orientation of a strike-slip event near the Kirkuk anticline (Fig. 2), as the event would be the right-lateral component of partitioned strain, acting with the thrusts to achieve the overall north-south plate convergence (Talebian and Jackson 2002).

A similar event occurred just to the southeast of Figure 2. It is notable that strike-slip faulting occurs across the Kirkuk Embayment, and is not restricted to the Main Recent Fault at the northeast margin of the Zagros, which is the case in the northwestern Iranian sector of the range. Two strike-slip focal mechanisms near the Himreen Anticline (Fig. 2) are not consistent with such right-lateral faulting, parallel to the fold trace. These earthquakes could relate to oblique cross faults on the anticline, not exposed at surface levels, as depicted by Kent (2010) for the Kirkuk Anticline.

The southwestern margin of the Kirkuk Embayment (Fig. 2) is the southwestern limit of the active deformation in the Zagros fold-and-thrust belt, which seems to be located at the transition between the pre-collisional stable and unstable shelf of the northern part of the Arabian Plate (Jassim and Goff 2006). It seems that the pre-collisional structure of the Arabian Plate exerts an influence on the extent of collisional deformation. In the Zagros fold-and-thrust belt several studies have interpreted unconformities as an indication of tectonic pulses (Farahpour and Hessami 2012; Hessami et al. 2001; Karim et al. 2011; Lawa et al. 2013) resulting in the step-wise progression of deformation towards the foreland. Given the diachronous nature of Cenozoic sedimentation in the region (e.g. Fakhari et al., 2008), and the possibility of unconformities being a response to base-level change and/or drainage re-organization, we consider that it is timely to re-evaluate these models for the Zagros tectonic evolution.

3. Methods and Data

3.1. Data

We have used the 90m DEM of Shuttle Radar Topography Mission (SRTM). The data have a specified vertical absolute accuracy of ≤16 m, and a vertical relative accuracy quoted as ≤10 m (Rodriguez et al. 2006 and references therein). These DEM data have been used in conjunction with satellite imagery, in particular Quickbird images. Geological maps (Sissakian 1993; Sissakian 1995; Zwaid 1993) were used for comparison with the exposed geology in each region. The MATLAB software toolkit TecDEM (Shahzad and Gloaguen 2011a,b) was used in combination with ArcGIS10.3.1 for data processing and the extraction of geomorphic indices. Part of the analysis is a simple qualitative investigation of the patterns of topography and drainage across the study area, including longitudinal river profiles. This inspection was performed to identify anomalous patterns, including topographic highs that might correspond to previously-unidentified folds and drainage diversion patterns and knickpoints that might correspond to zones of active deformation.

3.2. Geomorphic indices

This section describes the geomorphic indices used in the landscape analysis in this study (Fig. 4). The numerical ranges presented in Figures 5-7 are relative values, rather than absolute values that could be directly compared with other areas.

The Hypsometric Integral (HI) refers to the amount of surface above a given area and it highlights the elevated surfaces. When the HI is linked with the degree of dissection, it is considered to be a suitable parameter for detecting landscape evolution stages in the erosion cycle (Keller and Pinter 2002; Ohmori 1993; Strahler 1952). Low HI values are associated with dissected or more mature areas, while high values represent relatively youthful topography and less eroded areas (Keller and Pinter 2002; Pérez-Peña et al. 2009). For a given area, HI can be calculated using Equation 1 (Pike and Wilson 1971).

$$HI = \frac{H_{mean} - H_{min}}{H_{max} - H_{min}} \qquad (1)$$

Where H_{max}, H_{min}, and H_{mean} are the maximum, minimum, and mean elevations respectively (Fig. 4).

The surface roughness (SR), also known as vertical dissection, has been defined as the ratio between the analyzed topographic surface of an area and the area of flat topography, when the analyses are performed to the same geographic extent and constant elevation (Berti et al. 2013; Grohmann 2004; Hani et al. 2012). SR can be calculated using Equation 2. SR values close to 1.0 represent flat areas and the value increases as the surface becomes irregular.

$$SR = \frac{TS}{FS} \qquad (2)$$

Where SR is the surface roughness, TS is the analyzed topographic surface area, and FS is the corresponding horizontal area (Fig. 4).

Surface Index (SI) is the combination of both HI and SR characteristics which enables SI to be used to consider tectonic and erosion evolution, thereby determining the relative age of the landforms and the degree of dissection associated with them (Andreani et al. 2014; González et al. 2015). Uplifted surfaces become more irregular because of erosion as a result of rivers progressing toward their equilibrium state (Keller and Pinter 2002). Less mature landforms are therefore associated with high HI values and low SR values, and consequently, positive SI value. While more mature or more irregular surfaces associated with high SR values and low HI values and, therefore, negative SI values (Andreani et al. 2014; González et al. 2015). SI has been calculated as in Equation 3 (Andreani et al. 2014).

$$SI = \left(\frac{HI - HI_{min}}{HI_{max} - HI_{min}}\right) * \left(\frac{H - H_{min}}{H_{max} - H_{min}}\right) - \left(\frac{SR - SR_{min}}{SR_{max} - SR_{min}}\right) \quad (3)$$

Where HI, H, and, SR are the hypsometric integral, elevation, and surface roughness respectively. These parameters are converted automatically to a ratio using the minimum and maximum values for each raster datum (Andreani et al. 2014). SI has also been used in rock differentiation, by exploiting different erosion characteristics of different rocks (Othman and Gloaguen 2014). These indices are used in this paper to investigate landscape maturity and to explore whether the deformation has simply propagated from the northeast to the southwest, which would result in a consistent progression in the value of indices between anticlines in this direction if other factors are equivalent (e.g. climate, lithology), or if the situation is more complex.

For meaningful results of geomorphic indices the moving window should cover the whole width of the feature under study. The approximate width (half wavelength) of the anticlines in the Kirkuk Embayment is ~4000-5000 m. To address these features, we selected a 50 by 50 pixel moving window for the SRTM 90 m dataset, and a 150 by 150 pixel moving window for the SRTM 30 m dataset as optimal. These configurations are equally effective in picking out variations between the major structures in the study area (compare Fig. 7 and Supplementary Fig. 2I for example). A sensitivity analysis has been conducted, to investigate the robustness of the DEM analysis, and is presented in section 4.2.

4. Results

4.1 Morphotectonic Indices

Figure 5 and supplementary Figure 2C show the change in the HI value across the major structures in the Kirkuk Embayment. Low HI values are distributed across the QaraChauq anticline: in the range 0.14-0.17 for the SRTM 90 m dataset and 0.11-0.25 for the SRTM 30 m dataset. The HI values increase towards the south (0.35-0.5 for the SRTM 90 m and 0.34-0.0.55 for the SRTM 30 m), across an undulating area between the QaraChauq and Makhool anticlines. Further south, the HI value begins to decrease again (0.18-0.27 for the SRTM 90 m and 0.2-0.3 for the SRTM 30 m) along the Khanooqa, Makhool, and Himreen anticlines. To the north of QaraChauq Anticline, the HI values increase (0.29-0.41 for the SRTM 90 m and 0.3-0.41 for the SRTM 30 m) along the crest of the Kirkuk Anticline. As the HI values of the QaraChauq Anticline represent a relative low in the mapped area, it can be therefore identified as an area of higher landscape maturity if not an area of earlier uplift. In contrast, the HI values of the Kirkuk Anticline represent a relative high, identifying it as a less mature area. There is also a variation in SR values between the different folds (Fig. 6 and supplementary Fig. 2F). The QaraChauq Anticline shows the highest SR values (1.032-1.059 for the SRTM 90 m and 1.033-1.059 for the SRTM 30 m), and the Kirkuk Anticline shows the lowest values (1.0026-1.009 for the SRTM 90 m and 1.005-1.018 for the SRTM 30 m).

Building on these HI, and SR values, the SI index reveals different levels of landscape maturity and probably different times and /or rates of surface uplift (Fig. 7 and supplementary Fig. 2I). Negative SI values (-0.08 to -0.17 for the SRTM 90 m and -0.07 to -0.17 for the SRTM 30 m) occur across the QaraChauq Anticline, representing more mature and relatively highly dissected areas. Positive SI values (0.05-0.16 for the SRTM 90 m and 0.04 to 0.14 for the SRTM 30 m) are distributed across the surface of the Kirkuk Anticline representing relatively less mature and less dissected areas (Fig. 7 and supplementary).

An important question may be raised as to what differences across the study area lead to differences in the landscape maturity indices. To answer this question, three parameters need to be taken into consideration: climate, tectonic activity, and the variation in rock type (Burbank and Anderson 2002). First, it can be argued that the effect of the climate can be neglected as no noticeable regional climate variation is present on the scale of the study area in figures 5-7. Nor is it expected that differences in elevation between the anticlines could be the reason for the differences in the indices used: the differences in elevation do not exceed a few tens of meters between the studied anticlines (Fig. 2). Second, closer scrutiny of the geology of the anticlines shows that their outcrops consist of the same sequences of rock units (Kirkuk Group, Fat`ha, Injana, Mukdadiyah, and Bai Hassan formations). Whilst there are likely to be differences between the lithologies of these units, e.g. between resistant limestone of the Kirkuk Group and erodible siltstones of the Injana Formation, it is not recorded that any individual unit is highly variable on the scale of the study area. According to the independent study of Bretis et al (2011) these formations all have a similar resistance to erosion, except for the resistant limestones of the Kirkuk Group, which is only locally exposed on the crest of the QaraChauq Anticline (Fig. 3). If we exclude the exposures of the Kirkuk Group from our analysis it does not affect the overall results, as the area involved is <1% of the total study area.

Figure 3 shows the major exposure of the Injana Formation (Late Miocene) and minor exposure of the Fat`ha Formation (Middle Miocene) on the crest of the Kirkuk Anticline, while the majority of these formations have been removed from the crest of the QaraChauq Anticline and are exposed only on the flanks of the south and north QaraChauq and in the saddle between them. Kirkuk Group strata (Oligocene) are exposed on the south and north QaraChauq crests. In addition to the Kirkuk Group, the Euphrates Formation (Early Miocene) appears on the north QaraChauq crest, but is not found on the Kirkuk Anticline crest. The Fat`ha Formation is the major formation to be exposed on the Makhool and Himreen anticline crests. The Fat'ha Formation is older than the units exposed on the Kirkuk Anticline and younger than the formations exposed on the QaraChauq Anticline.

From the above discussion it can be inferred that the climate and rock type have no effect on the variation in the calculated geomorphic indices across the area of Fig. 3 as a whole. Tectonic effects should therefore be the controlling factor on the geomorphic indices, but this includes both the age of the structures and their rock uplift rates.

Using the variation in SI values (Fig. 7), and the age of the exposed geology on the crests of anticlines in the Kirkuk Embayment, it can be concluded that the main anticlines formed in the order of S. QaraChauq, N. QaraChauq, Makhool, Himreen, and lastly Kirkuk, which is the order of increasing SI value. According to the thinning over anticline crests recorded in the Mukdadiyah Formation, which reflects syn-tectonic deposition, folding in the Kirkuk Embayment started in a short period in the Late Miocene (Fig. 15b in Kent 2010). This means that the deformation of the prominent structures in the Kirkuk Embayment is a late Cenozoic phenomenon.

4.2 Sensitivity analysis

Errors and uncertainties related to the original DEM quality and resolution are inevitable, and analytical methods attempt to reduce these errors (Kirby and Whipple 2012). In this section we explore the effects of using different moving windows for the three indices, using both the 90 m and 30 m SRTM data.

If the moving window covers too small an area, it highlights local features related to drainage patterns, which obscure the signals from the main anticlines. If the moving window is too large, the anticlines themselves are not successfully resolved. Supplementary Figure 2 gives examples of both of these phenomena.

The extra processing time required for the SRTM 30 m data is a reason not to use this dataset. Again, we stress that the intention of our study is to investigate variations in landscape maturity on the scale of the major anticlines. In this context, the extra resolution of the 30 m data is of no advantage.

For all the three indices (HI, SR and SI) the 90 m and the 30 m SRTM datasets have ranges which are different from each other by <0.08, across the major anticlines in the Kirkuk Embayment. The subtlest variations in the studied landscape which seem to have a real tectonic significance are on the order of 0.02 units in the SI diagram (Fig. 7); see section 4.4.

4.3 Lesser Zab interactions with folds

The Lesser Zab is the main river in the study area (Figs. 2 and 3). It runs northeast-southwest across the anticlines discussed above. The river maintains a distinctly straight course across the Kirkuk, Bai Hassan and QaraButak anticlines (Fig. 3) without showing clear knickpoints (Fig. 8). Nor is there a knickpoint associated with either of the newly-identified folds which are described in the next section. None of these anticlines is appreciably offset in either horizontal or vertical dimensions; there is no evidence that a reactivated basement structure runs along the length of the Lesser Zab, as has been indicated in some previous tectonic maps of the region (e.g. Burberry, 2015), cross-cutting anticlines such as Kirkuk. The Lesser Zab joins the Tigris, ~10 km north of the Makhool Anticline, and the combined river flows another ~20 km to the SE before crossing the Makhool Anticline at its termination, which is also the relay zone with the tip of the Himreen Anticline. The junction of the Makhool and Himreen anticlines is an example of the kind of en echelon fold linkage described by Bretis et al (2011) northeast of the Kirkuk Embayment in the Iraqi Zagros, in this case exploited by the Tigris River. Figure 9 shows that the Tharthar trough, south of the Makhool Anticline, could be the original continuation of the course of the Tigris River, if the Makhool Anticline had not developed. As rivers tend in nature to gravitate towards the zones of subsidence when there is no topographic barrier (Holbrook and Schumm, 1999), the Tharthar trough would represent a pathway for the Tigris, rather than diverting eastwards across the nose of Makhool Anticline as it does now. The modern drainage in the Tharthar trough seems distinctly misfit, as though at an earlier time the trough was occupied by a much larger river (see the cross-valley profiles in Figure 9).

According to the discharge data (Saleh, 2010) the stream power of the Tigris River (Fig. 8) before approaching the Makhool anticline is 27,400 kg.m/s^3 (and a near-constant gradient of 0.004). The Lesser Zab River crosses the Kirkuk, Bai-Hassan, and QaraButak anticlines with a straight flow path, near-constant gradient (0.007) and stream power of 16,900 kg.m/s^3. The two rivers combine north of the Makhool Anticline, but, unlike the behaviour of the Lesser Zab to the north, even the combined rivers are diverted eastwards by the growth of the Makhool Anticline, before flowing across the nose of the fold.

The cross-cutting relationships between the Lesser Zab River and the anticlines in the Kirkuk Embayment can be interpreted to give a scenario about the sequence of anticlinal growth in this area. The Lesser Zab River crosses the Kirkuk and Bai Hassan anticlines (which are relatively less mature according to the surface index), while it diverts around the nose of the Makhool anticline (which is relatively more mature). There is no noticeable change in gradient along Lesser Zab River profile (Fig. 8). Thus, the Lesser Zab River overcomes the growth of the Kirkuk and Bai Hassan anticlines, and the river crosses these anticlines without deflections, wind gaps or knickpoints. However, it appears that the Makhool Anticline exceeded the ability of the combined Lesser Zab and Tigris River to cut through the growing fold, and consequently the river was diverted by the fold; this relationship could mean faster growth of Makhool than the folds to the north, but may mean that the palaeo-gradient was lower before the uplift of structures to the north. Note that Koshnaw et al. (2017) put the initiation of the Kirkuk Anticline during the deposition of the Mukdadiyah Formation in the Late Miocene, based on syn-fold strata of this age on the south side of the anticline; their data come from an area ~100 km southeast of ours, so there is the potential for different sectors of the same fold to be of different ages due to lateral fold growth.

4.4 Identification of incipient folding

The broad synclinal area between the Kirkuk and Himreen anticlines is covered by Holocene sediments (Jassim and Goff 2006). Published structural maps typically show a gap between the QaraChauq Anticline and the Himreen Anticline with no fold structures in this region (e.g. Fouad 2015; Burberry et al. 2015; Koshnaw et al., 2017; Fig. 3). Figure 10 shows two subdued topographic rises within this area, both trending northwest-southeast, in parallel with the regional fold trend. The spacing between these rises is ~20 km, which is similar to the spacing between at least some of the well-developed folds in the Iraqi Zagros, such as QaraChauq and Kirkuk (Fig. 3). Four topographic profiles have been drawn perpendicular to the hinge lines of the Khderat Anticline (on the flank of the adjacent Makhool Anticline), and the two newly-identified rises. These profiles show the similarity in half wavelength and amplitude of the three structures (Fig. 10). It can be seen that the northeastern rise is similar in relative elevation to the Khderat Anticline (Fig. 10). The SI values show isolated areas of positive values that could represent youthful topography and uplifted surfaces, with a difference of ~0.02 in the SI value between the rises and adjacent areas. These areas between the QaraChauq and Makhool anticlines are represented by the orange color in the SI map (Fig. 7).

Drainage patterns were also analysed as an indication of uplift, and show a radial pattern that reflects a dome-shaped topography (Fig. 11). Tracing the drainage network configuration shows clearly the occurrence of elongated and low relief structures in a consistent pattern with the youthful topography highlighted by SI contours (Fig. 7). The notable advantage of the drainage network analysis is that it shows both crests to the east of the Lesser Zab River, with a clarity that is not present in the morphotectonic indices or the raw topographic data. These features are similar in their linkage and orientation with QaraChauq/QaraButak anticlines. In addition, seismicity data shows a thrust earthquake (Fig. 2 and Fig. 10) with a depth of ~20 km occurred in 2013 in the vicinity of this uplifted topography.

Based on the topography, drainage patterns, and HI and SI values, these two rises between the QaraChauq and Himreen anticlines are interpreted to represent low relief anticlines that are growing due to the activity of thrust faults at depth, evidenced by the seismicity in the region. We informally named the two rises according to the names of the nearest villages as i) Halwah, which the northern rise towards QaraChauq (Fig. 12), and ii) Shariyah, which is the southern rise, closer to Makhool. These structures have not previously been mapped in the Iraqi geological survey publications (e.g. Fouad 2015; Sissakian 2000). The Halwah and Shariyah structures might be of importance as 4-way closure anticlines that trap oil and/or gas, like the existing oil and gas fields distributed in the area.

Further southwest of the Zagros belt, in the Baghdad Oil Field (central Iraq), seismic interpretation has demonstrated the presence of subsurface large scale block-faulted structures with lengths over 120 km and 20-30 km width. These are present from Baghdad (central Iraq), Balad, Samarra, and Tikrit towards the northwest **(**Aqrawi et al. 2010 and reference therein**)**. These structures were deformed by wrench faulting in Late Cretaceous (Cenomanian) and they have internal horst and graben and flower structures, as described by Kent (2010) for the Makhool/Khanooqa, Kirkuk/Bai Hassan, and Mansuriya structures. This Cretaceous deformation took place in the foreland to the present Zagros, i.e. the deformation front related to the continental collision has not reached as far southwest as the deformation related to the Cretaceous obduction of ophiolites onto the Arabian margin. In addition, Aqrawi et al. (2010) i.e. their Figs. 5 and 6, and Mohammed (2006) i.e. his Fig. 8, show that steeply dipping basement faults control the deformation of Paleozoic, Mesozoic, and Cenozoic sequences for the whole area of the northwestern Zagros. It is probable that differential rates of movement of these basement faults might control the uplift of anticlines towards the foreland, but the onset of late Cenozoic activity did not occur in sequence towards the foreland.

4.5 Balanced cross-section

We have used previously published data for the region in conjunction with our own analysis to construct a new cross-section across the Kirkuk Embayment (Fig. 13). Outcrop constraints, including dip and strike data, are extrapolated from fieldwork observations at the east of the Kirkuk Embayment, which will be reported in detail elsewhere. In particular, this section utilizes the detailed sub-surface data shown by Kent (2010) in a cross-section for the Mansuriya

Anticline, which is located to the southeast of our study area, along strike from the Himreen Anticline (Fig. 2). Relevant aspects of the Mansuriya Anticline structure include: localized detachment within the Fat'ha Formation (consistent with the small-scale deformation features seen in field photographs in the supplementary file); underlying thrust faults that penetrate below the Mesozoic section towards the basement (consistent with seismicity evidence for the Zagros, Nissen et al., 2011); stratigraphic evidence for Cretaceous extensional faulting and subsequent inversion; divergent thrust faults underlying fold crests and possible flower structure geometries.

We use the regional seismicity record as a further guide to the general structural style, without over-reliance on any single event. In particular, the nodal planes for the earthquakes in the Iraqi Zagros are relatively steep (>30^{o}), regardless of which is the real and which is the auxiliary plane; this observation is consistent across the great majority of M >5 earthquakes in the Zagros (Nissen et al., 2011). We depict the thrust faults on Figure 13 in keeping with this observation. If there is a low-angle detachment thrust beneath the Zagros, it is aseismic. Alternatively, no such thrust exists.

Our section in essence repeats these structural styles across the Kirkuk Embayment anticlines (for which there are limited subsurface data), and furthermore incorporates the Halwah and Shariyah structures between the QaraChauq and Makhool/Himreen anticlines. These folds, albeit modest in size, occupy what would otherwise be a gap in the Embayment, and mean that the typical spacing between folds (and their underlying thrusts) is ~20 km (Figure 13).

5. Discussion

Three possible hypotheses might be envisaged in relation to fold growth, based on the variation in SI values and other geomorphic indices (Figs. 5-7). First, it may be that the folds grew out of sequence (in the order of initiation: QaraChauq, Makhool, Himreen, Kirkuk, and finally Halwah and Shariyah), and at different times (Fig. 12). Second, the folds grew all at the same time, but with different rates of exhumation. Both of these scenarios mean that the progression of deformation was not simply from the northeast to the southwest. Third, the folds grew in sequence towards the foreland, but with different rates of exhumation, to produce the observed variation in geomorphic indices. This seems the most complicated arrangement, and therefore the least likely. On the basis of all the above-discussed evidence, we conclude that the deformation in the Kirkuk Embayment does not follow simple foreland progression of deformation from the northeast to the southwest. Possibly, the arrangement and the apparent order of activity (Fig. 12) might be attributed to the activity of basement faults, available for reactivation during the late Cenozoic compressional deformation.

Koshnaw et al (2017) also interpreted out-of-sequence thrusting and fold growth in another area of the Iraqi Zagros, southeast of our study area, based on the different ages of syn-fold growth strata within the fold-and-thrust belt; their conclusion is entirely consistent with our independent observations of the same phenomenon, based on the landscape maturity indices. Where we differ from the interpretation of Koshnaw et al. (2017) is that we do not regard the later structures as the only ones to be basement-involved, but interpret all of the main thrusts to be thick-skinned.

Flower structures are present in the Mansuriya oil field (MOF) to the east of the Kirkuk Embayment (Fig. 2), and the Jebissa/Sinjar anticlines and Butmah/Ain Zalah anticlines to the northwest of the Kirkuk Embayment. These structures were interpreted as reactivated graben structures which is also a good interpretation for the occurrence of pairs of folds such as Kirkuk/Bai Hassan, and Makhool/Khanooqa (Kent 2010). It can be inferred that Halwah and Shariyah anticlines are other examples of flower structures in the region. The distributed strike-slip earthquakes across the Kirkuk Embayment (Fig. 2) are another suggestion of flower structure development across the region, i.e. many of the folds expressed at the surface as linear anticlinal ridges may have a strike-slip component, not obvious in the shallow geology. An implication of this result is that the strain partitioning of north-south Arabia-Eurasia plate convergence does not occur via a single strike-slip fault, as is the case further to the southeast (Talebian and Jackson, 2004), but is instead partly distributed across a family of structures within the Kirkuk Embayment.

The spacing between anticline crests is ~20 km (Fig. 13), identified through the discovery of the Halwah and Shariyah anticlines by analysis of the drainage patterns and geomorphic indices. The length of many fold segments is similar (Fig. 3), although there are also long, linear sections of folds such as the Kirkuk Anticline where no such segmentation has yet been identified; see Koshnaw et al (2017), Figure 3. This 20 km figure is notable for being similar to the length and separation of Zagros fold segments identified to the southeast, in the Iranian sector of the range (Ramsey et al. 2008). Both the length and across-strike spacing of the folds (and inferred underlying faults) may relate to the distribution of pre-Cenozoic normal faults within the Arabian Plate, reactivated as thrusts by the Cenozoic collision (Ramsey et al. 2008).

The amount of late Cenozoic shortening across the new cross-section is relatively small, in the order of 5%, which is roughly 5 km across the 100 km section line (Fig. 13). It is consistent with the pattern of narrow anticlines, separated by wide regions of essentially undeformed strata and levels of exhumation typically no deeper than the Neogene. This result is therefore no surprise, but emphasizes the likelihood that strain is not evenly distributed across the Zagros, in the embayments and the adjacent regions to their northeast. In this respect, the pattern of deformation in the Kirkuk Embayment is similar to the Dezful Embayment to the southeast. It is very important to use high resolution seismic data to investigate the distribution of basement faults and to understand the deformation in the Cenozoic strata. This will serve the oil exploration and also help in understanding the structural evolution of the northwest Zagros.

6. Conclusions

In this paper geomorphic surface indices provide new insights on the nature of anticline growth in the Kirkuk Embayment, by revealing different degrees of landscape maturity. It can be inferred that the Zagros fold and thrust belt does not follow a simple progression from the northeast towards the foreland over time (Fig. 12). More mature anticlines are located in the southwest, and the less mature ones in the northeast, such as the Makhool and Kirkuk anticlines respectively.

There are broader implications of this result for the evolution of the Zagros, and fold-and-thrust belts in general, which is that simple models for the foreland propagation of deformation, possibly in a critical wedge framework, may not be correct. The departure from such models in the Kirkuk Embayment may relate to northwest-southeast trending basement faults in the region; these faults promote out-of-sequence reactivation, dependent on the ease with which fault slip occurs on each individual structure, rather than regional stresses arising from a critically tapered wedge.

Late Cenozoic shortening across the Kirkuk Embayment is small, in the order of 5%, or ~5 km in the section line from the Kirkuk Anticline to the deformation front to the southwest (Fig. 13). Topographic analysis, drainage patterns and the Surface Index parameter reveal two previously-unrecorded anticlines, which might be possible traps of oil and gas in the region. Acquisition and analysis of more seismic data is recommended, to investigate the sub-surface structure.

Acknowledgments

We thank the Ministry of Higher Education and Scientific Research in Iraq for their support of the first author's project. We thank Chris Saville for useful discussion of the geomorphic indices. The authors thank Dr. Arsalan Ahmed Othman, for his review and valuable field information. The development team of the software TecDEM is highly appreciated. We thank two anonymous referees for their helpful reviews.

References

Alavi, M., 2007. Structures of the Zagros fold-thrust belt in Iran. American Journal of Science 307, 1064–1095.

Alipoor, R., Pourkermani, M., Zare, Mm., El Hamdouni, R., 2011. Active tectonic assessment around Rudbar Lorestan dam site, High Zagros Belt (SW of Iran). Geomorphology 128, 1–14.

Allen, M. B., Saville, C., Blanc, E. J-P, Talebian, M., Nissen, E., 2013. Orogenic plateau growth: Expansion of the Turkish-Iranian Plateau across the Zagros fold-and-thrust belt. Tectonics 32, 171–190.

Allen, M. B., Armstrong, H. A., 2008. Arabia-Eurasia collision and the forcing of mid- Cenozoic global cooling. Palaeogeography, Palaeoclimatology, Palaeoecology 265, 52–58.

Allen, M. B., Talebian, M., 2011. Structural variation along the Zagros and the nature of the Dezful Embayment. Geological Magazine 148, 911–924.

Ameen, M. S., 1992. Effect of basement tectonics on hydrocarbon generation, migration, and accumulation in Northern Iraq. American Association of Petroleum Geologists Bulletin 76, 356–370.

Andreani, L., Stanek, P. K., Gloaguen, R.,Krentz, Ottomar, Dominquez-Gonzalez, L., 2014. DEM-Based Analysis of Interactions between Tectonics and Landscapes in the Ore Mountains and Eger Rift (East Germany and NW Czech Republic). Remote Sensing 6, 7971–8001.

Aqrawi,A. M., Goff, J.C., Horbury, A.D., Sadooni, F.N., 2010. The Petroleum Geology of Iraq, First ed. Scientific Press Ltd, Aberystwyth.

Bagha, N., Arian, M., Ghorashi, M., Pourkermani, M., El-Hamdouni,.R., Solgi, A., 2014. Evaluation of relative tectonic activity in the Tehran basin, central Alborz, northern Iran. Geomorphology 213, 66–87.

Bahrami, S., 2012. Morphotectonic evolution of triangular facets and wine-glass valleys in the Noakoh anticline, Zagros, Iran: Implications for active tectonics. Geomorphology 159–160, 37– 49.

Bahrami, S., 2013. Analyzing the drainage system anomaly of zagros basins: Implications for active tectonics. Tectonophysics 608, 914–928.

van Bellen, R. C. et al., 1956. Stratigraphic Lexicon of Iraq. CNRS, Paris.

Berberian, M., 1995. Master “blind” thrust faults hidden under the Zagros folds: active basement tectonics and surface morphotectonics. Tectonophysics 241, 193–224.

Berti, M., 2013. Copmarative analysis of surface roughness algorithms for the identification of active landslides. Geomorphology 182, 1–18.

Blanc, E. J.-P., Allen, M. B., Inger, S., Hassani, H., 2003. Structural styles in the Zagros Simple Folded Zone, Iran. Journal of the Geological Society 160, 401–412.

Bretis, B., Bartl, N., Grasemann, B., 2011. Lateral fold growth and linkage in the Zagros fold and thrust belt (Kurdistan, NE Iraq). Basin Research 23, 615–630.

Burbank, D. W., Anderson, R. S. 2002. Tectonic geomorphology, second ed. Wiley-Blackwell, USA.

Burberry, C. M. 2015. The effect of basement faults reactivation on the Triassic-Recent geology of Kurdistan , North Iraq. Journal of Petroleum Geology 38, 37–58.

Dehbozorgi, M., Pourkermani, M., Arian, M., Matkan, A. A., Motamedi, H., Hosseiniasl, A., 2010. Quantitative analysis of relative tectonic activity in the Sarvestan area, central Zagros, Iran. Geomorphology 121, 329–341.

Domínguez-González, L., Andreani, L., Stanek, K. P., Gloaguen, R.,, 2015. Geomorpho-tectonic evolution of the Jamaican restraining bend. Geomorphology 228, 320–334.

Dunnington, H. V. 1958. Generation, migration, accumulation and dissipation of oil in Northern Iraq. Journal of Petroleum Geology (special publications), 1192–1251.

Ehsani, J., Arian, M., 2015. Quantitative analysis of relative tectonic activity in the Jarahi-Hindujan basin area, Zagros, Iran. Geosciences Journal. DOI:10.1007/s12303-015- 0016–3

El Hamdouni, R., Irigaray, C., Fernandez, T., Chacon, J., Keller, E. A., 2008. Assessment of relative active tectonics, southwest border of the Sierra Nevada (southern Spain). Geomorphology 96, 150 –173.

Fakhari, M.D., Axen, G. J., Horton, B.K., Hassanzadeh, J., Amini, A. , 2008. Revised age of proximal deposits in the Zagros foreland basin and implication for Cenozoic evolution of the High Zagros. Tectonophysics, 451, 170–185.

Farahpour, M. M., Hessami, K., 2012. Cretaceous sequence of deformation in the SE Zagros fold-thrust belt. Journal of the Geological Society 169, 733–743.

Fard, N. G., Sorbi, A., Arian, M., 2015. Active Tectonics of Kangavar Area. Open Journal of Geology 5, 422–441.

Font, M., Amorese, D., Lagarde, J. L., 2010. DEM and GIS analysis of the stream gradient index to evaluate effects of tectonics: The Normandy intraplate area (NW France). Geomorphology 119, 172–180.

Fouad, S., 2015. Tectonic map of Iraq, scale 1:1000,000. Iraqi Bulletin of Geology and Mining 11, 1–7.

Ghasemi, A., Talbot, C., 2006. A new tectonic scenario for the Sanandaj-Sirjan Zone (Iran). Journal of Asian Earth Sciences 26, 683–693.

Grohmann, C. H., 2004. Morphometric analysis in geographic information systems: Applications of free software GRASS and R. Computers and Geosciences 30, 1055– 1067.

Hani, A. F., Sathyamoorthy, D., Asirvadam, V. S., 2012. Computing surface roughness of individual cells of digital elevation models via multi scale analysis. Computers & Geosciences 43, 13–146.

Hessami, K., Koyi, H. A., Talbot, C. J., Tabasi, H., Shabanian, E., 2001. Progressive unconformities within an evolving foreland fold-thrust belt, Zagros Mountains. Journal of the Geological Society 158, 969–981.

Holbrook, J., Schumm, S. A., 1999. Geomorphic and sedimentary response of rivers to tectonic deformation: a brief review and critique of a tool for recognizing subtle epeirogenic deformation in modern and ancient settings. Tectonophysics 305, 287–306.

Jassim, S. Z., Goff, J.C., 2006. Geology of Iraq, first ed. Dolin Prague and Moravian Museum, Prague (341pp).

Karim, K. H. Koyi, H., Baziani, M. M., Hessami, K., 2011. Significance of angular unconformities between Cretaceous and Tertiary strata in the northwestern segment of the Zagros fold–thrust belt, Kurdistan Region, NE Iraq. Geological Magazine 148, 925–939.

Keller, E. , Pinter, N., 2002. Active Tectonics: Earthquakes,Uplift, and Landscape. Prentice Hall, New Jersey.

Kent, W. N., 2010. Structures of the Kirkuk Embayment, northern Iraq: Foreland structures or Zagros Fold Belt structures? GeoArabia 15, 147–188.

Kirby, E., Whipple, K. X., 2012. Expression of active tectonics in erosional landscapes. Journal of Structural Geology 44, 54–75.

Koshnaw, R.I., Horton, B.K., Stockli, D.F., Barber, D.E., Tamar-Agha, M.Y., Kendall, J.J., 2017. Neogene shortening and exhumation of the Zagros fold-thrust belt and foreland basin in the Kurdistan region of northern Iraq. Tectonophysics 694, 332–355.

Lawa, F., Koyi, H., Ibrahim, A., 2013. Tectono-stratigraphic evolution of the NW segment of the Zagros fold-thrust belt, Kurdistan, NE Iraq. Journal of Petroleum Geology 36, 75–96.

Mahmood, S. A., Gloaguen, R., 2012. Appraisal of active tectonics in Hindu Kush: Insights from DEM derived geomorphic indices and drainage analysis. Geoscience Frontiers 3, 407– 428.

McQuarrie, N., Stock, J.M., Verdel,C., Wernicke, B.P., 2003. Cenozoic evolution of the Neotethys and implication for the causes of plate motions. Geophysicsal Research Letters 30, 2036.

McQuarrie, N., 2004. Crustal scale geometry of the Zagros fold-thrust belt, Iran. Journal of Structural Geology. 26, 519–535.

McQuarrie, N., van Hinsbergen, D. J., 2013. Retrodeforming the Arabia-Eurasia collision zone: Age of collision versus magnitude of continental subduction. Geology 41, 315–318.

Mohammed, S., 2006. Megaseismic section across the northeastern slope of the Arabian Plate, Iraq. GeoArabia 11, 77–90.

Mosavi, E. J. Arian, M., Ghorshi,M., Nazemi, M., 2015. Neotectonics of Tabas Area, Central Iran by Index of Active Tectonics (IAT). Open Journal of Geology 5, 209–223.

Mouthereau, F., Lacombe, O., Vergés, J., 2012. Building the Zagros collisional orogen: timing, strain distribution and the dynamics of Arabia/Eurasia plate convergence. Tectonophysics 532, 27–60.

Nissen, E. Tatar, M., Jackson, J. A., Aleen, M. B., 2011.New views on earthquake faulting in the Zagros fold-and-thrust belt of Iran. Geophysical Journal International 186, 928–944.

Ohmori, H., 1993. Changes in the hypsometric curve through mountain building resulting from concurrent tectonics and denudation. Geomorphology 8, 263–277.

Othman, A., Gloaguen, R., 2014.Improving Lithological Mapping by SVM Classification of Spectral and Morphological Features: The Discovery of a New Chromite Body in the Mawat Ophiolite Complex (Kurdistan, NE Iraq). Remote Sensing 6, 6867– 6896.

Pérez-Peña, J. V. et al., 2009. Differentiating geology and tectonics using a spatial autocorrelation technique for the hypsometric integral. Journal of Geophysical Research: Earth Surface 114, 1–15.

Pike, R. J., Wilson, S. E., 1971. Elevation-relief ratio, hypsometric integral, and geomorphic area-altitude analysis. Bulletin of the Geological Society of America 82, 1079–1084.

Ramsey, L. A., Walker, T., Jackson, J., 2008. Fold evolution and drainage development in the Zagros mountains of Fars province , SE Iran. Basin Research 20, 23– 48.

Rodriguez, E., Morris, C., Belz, J., 2006. A global assessment of the SRTM perfor-mance. Photogrammetric Engineering and Remote Sensing 72, 249–260.

Saleh, D. K., 2010. Stream gage descriptions and streamflow statistics for sites in the Tigris River and Euphrates River Basins, Iraq. U.S. Geological Survey Data Series 540, 7–108.

Shahzad, F., Gloaguen, R., 2011a. TecDEM: A MATLAB based toolbox for tectonic geomorphology, Part 1: Drainage network preprocessing and stream profile analysis. Computers and Geosciences 37, 250–260.

Shahzad, F., Gloaguen, R., 2011b. TecDEM: A MATLAB based toolbox for tectonic geomorphology, Part 2: Surface dynamics and basin analysis. Computers and Geosciences 37, 261–271.

Siddiqui, S., 2014. Appraisal of Active Deformation Using DEM-based Morphometric Indices Analysis in Emilia-Romagna Apennines, northern Italy. Geodynamics Research International Bulletin 1, 34– 42.

Singh, T., Jain, V., 2009. Tectonic constraints on watershed development on frontal ridges: Mohand Ridge, NW Himalaya, India. Geomorphology 106, 231–241.

Sissakian, K. V., 1993. The Geology of Kirkuk Quadrangle sheet No. NI–38–2, Scale 1:250,000. GEOSURV, Baghdad, Iraq.

Sissakian, K. V., 1995. The Geology of AL-Mosul Quadrangle sheet No. NJ–38–13, Scale 1:250,000. GEOSURV, Baghdad, Iraq.

Stern, R. J., Johnson, P., 2010. Continental lithosphere of the Arabian Plate: A geologic, petrologic, and geophysical synthesis. Earth-Science Reviews 101, 29–67.

Strahler, A., 1952. Hypsometric (area-altitude) analysis of erosional topology. Bulletin of the Geological Society of America 63, 1117–1142.

Talebian, M., Jackson, J., 2004. A reappraisal of earthquake focal mechanisms and active shortening in the Zagros mountains of Iran. Geophysical Journal International 156 , 506–526.

Talebian, M., Jackson, J., 2002. Offset on the Main Recent Fault of NW Iran and implications for the late Cenozoic tectonics of the Arabia-Eurasia collision zone. Geophysical Journal International 150, 422–439.

Vera, J., De Gines, J., 2009. Structure of the Zagros fold and thrust belt in the Kurdistan Region, northern Iraq. Trabajos de Geología, Universidad de Oviedo 29, 213–217.

Vergés, J.Saura, E., Casciello, E., Fernandez, M., Villasenor, A., Jimenez-Mount, I., Garcia-Castellanos, D., 2011. Crustal-scale cross-sections across the NW Zagros belt: implications for the Arabian margin reconstruction. Geological Magazine 148, 739–761.

Vernant, P., Nilforoushan, F., Hatzfel, D., Abbassi, M. R., Vigny, C., Masson, F., Nankali, H., Matinod, J., Ashtiani, A., Bayer, R., Tavakoli, F., Chery,J., 2004. Present-day crustal deformation and plate kinematics in the Middle East constrained by GPS measurements in Iran and northern Oman. Geophysical Journal International 157, 381–398.

Zwaid, A. Q., 1993.The Geology of AL-Qaiyara Quadrangle sheet No. NI–38–1, Scale 1:250,000. GEOSURV, Baghdad, Iraq.

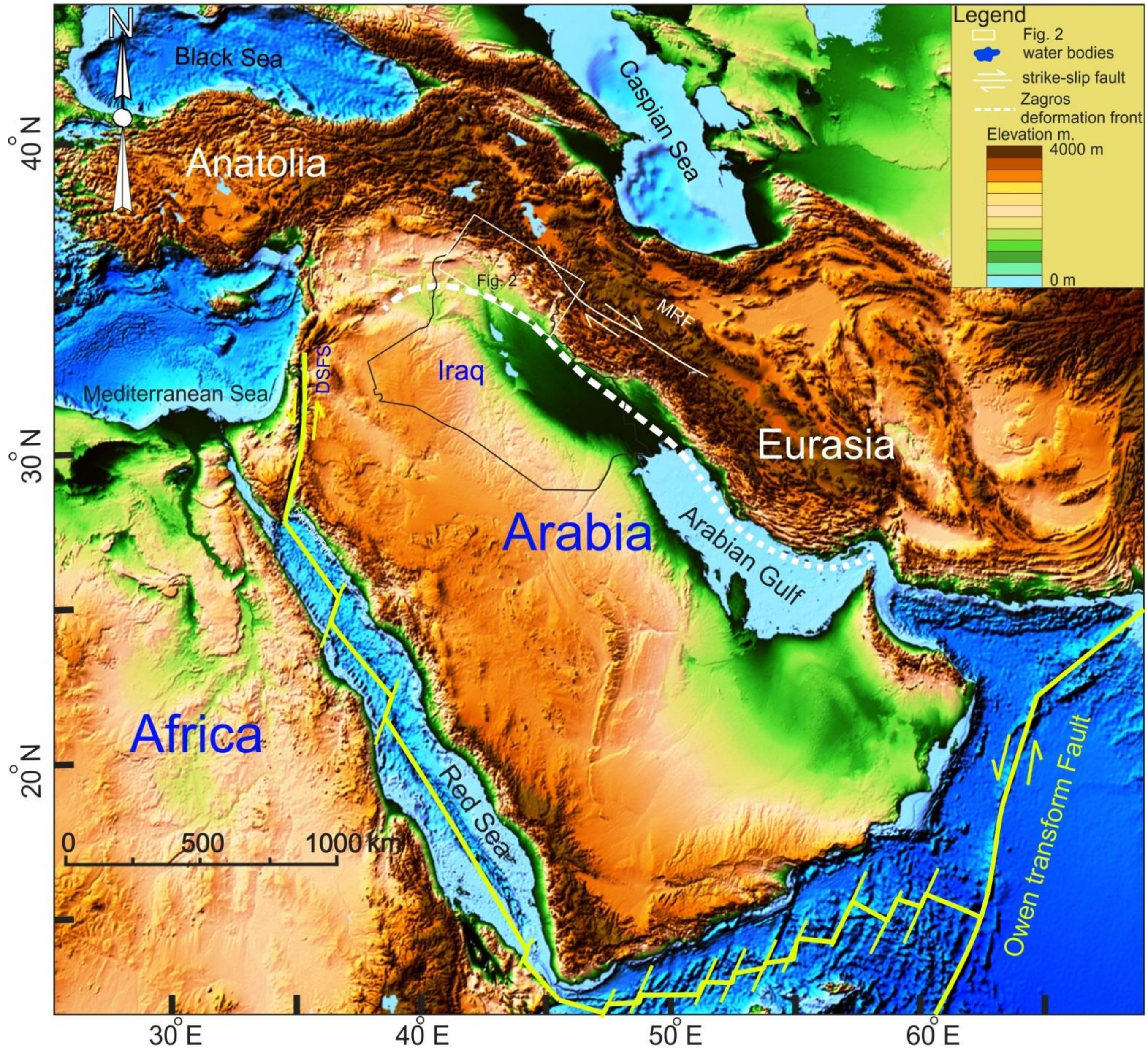

Fig. 1. ETOPO1 Global Relief Model (National Geophysical Data Centre), showing the regional tectonics of the Arabia-Eurasia collision. The dashed white line is the approximate position of the deformation front of the Arabia-Eurasia collision. Abbreviation: MRF, Main Recent Fault; DSFS, Dead Sea Fault System.

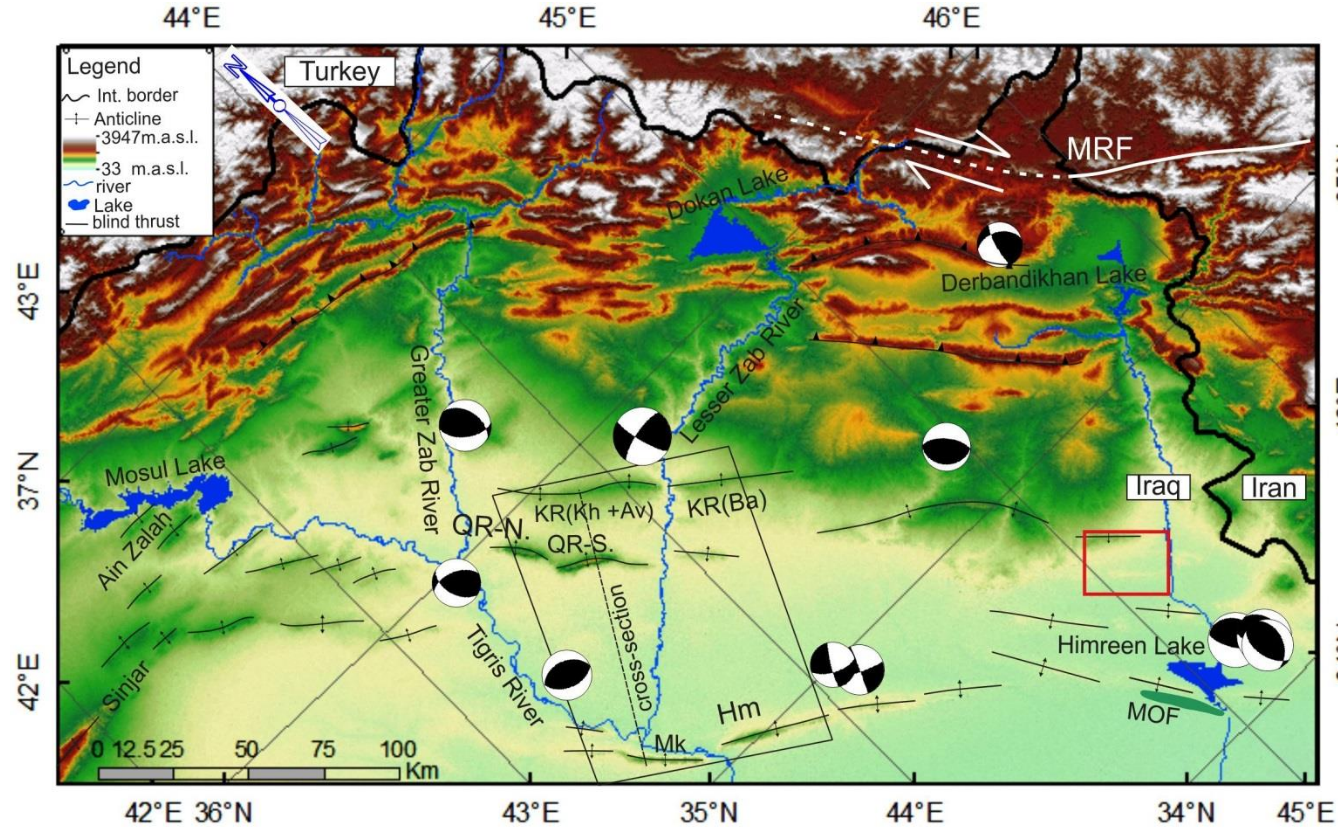

Fig. 2. Structural map of the northwest part of the Zagros fold and thrust belt. QR-N, QaraChauq North; QR-S, QaraChauq South; KR (Kh.+Av.), Kirkuk (Khurmala and Avanah); KR (Ba), Kirkuk (Baba); Mk, Makhool; Hm, Himreen; MOF, Mansuriya Oil Field. Focal mechanisms are adapted from the Global CMT catalogue, and show the widespread distribution of thrust faulting. The black box shows the location of Figs. 3, 5-7 and 11. The red box shows the location of the field photographs in the supplementary figure 1.

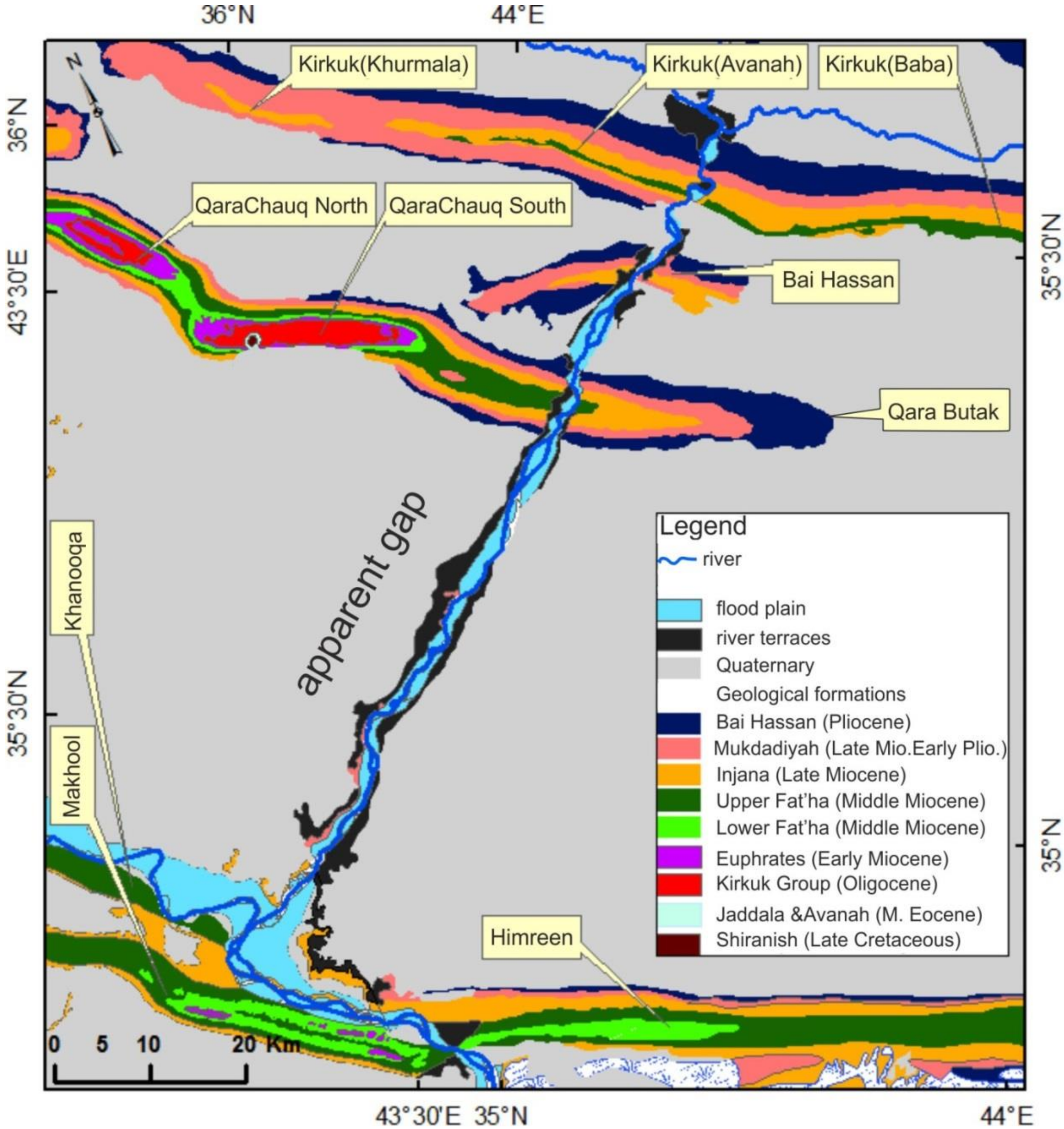

Fig. 3. Geological map of the NW part of the Kirkuk Embayment (Sissakian 1993; Sissakian 1995; Zwaid 1993). The Kirkuk Group is the main hydrocarbon reservoir in the region, which is mostly limestone. The Fat'ha Formation is mainly anhydrite, with prominent marls and clay layers in its upper part. The Injana Formation consists of a variety of non-marine clastic sediments. The Mukdadiyah Formation consists dominantly of sandstone. The Bai Hassan Formation consists of very coarse–grained conglomerate, with sandstone and clays dominantly in the lower part of the formation.

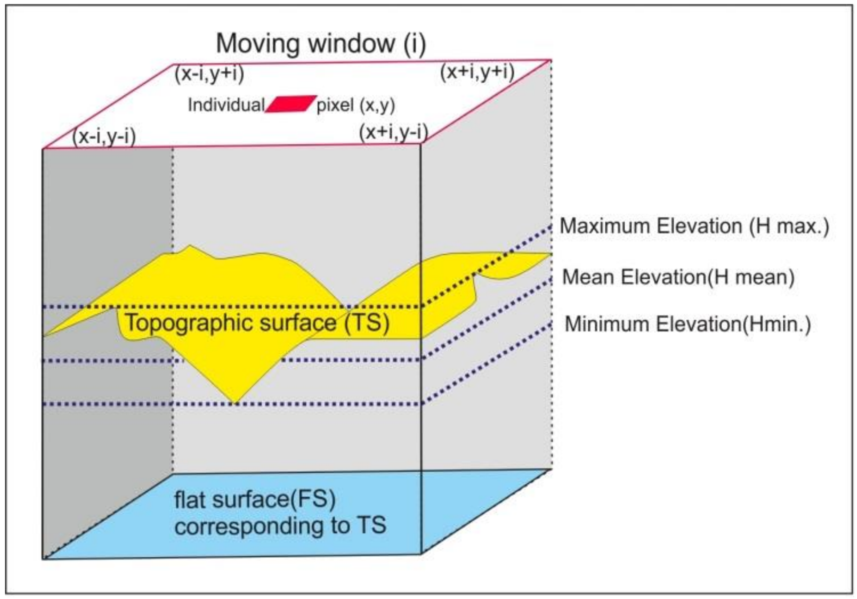

Fig. 4. Sketch diagram shows the basic of HI and SR calculation (modified after Andreani et al. 2014).

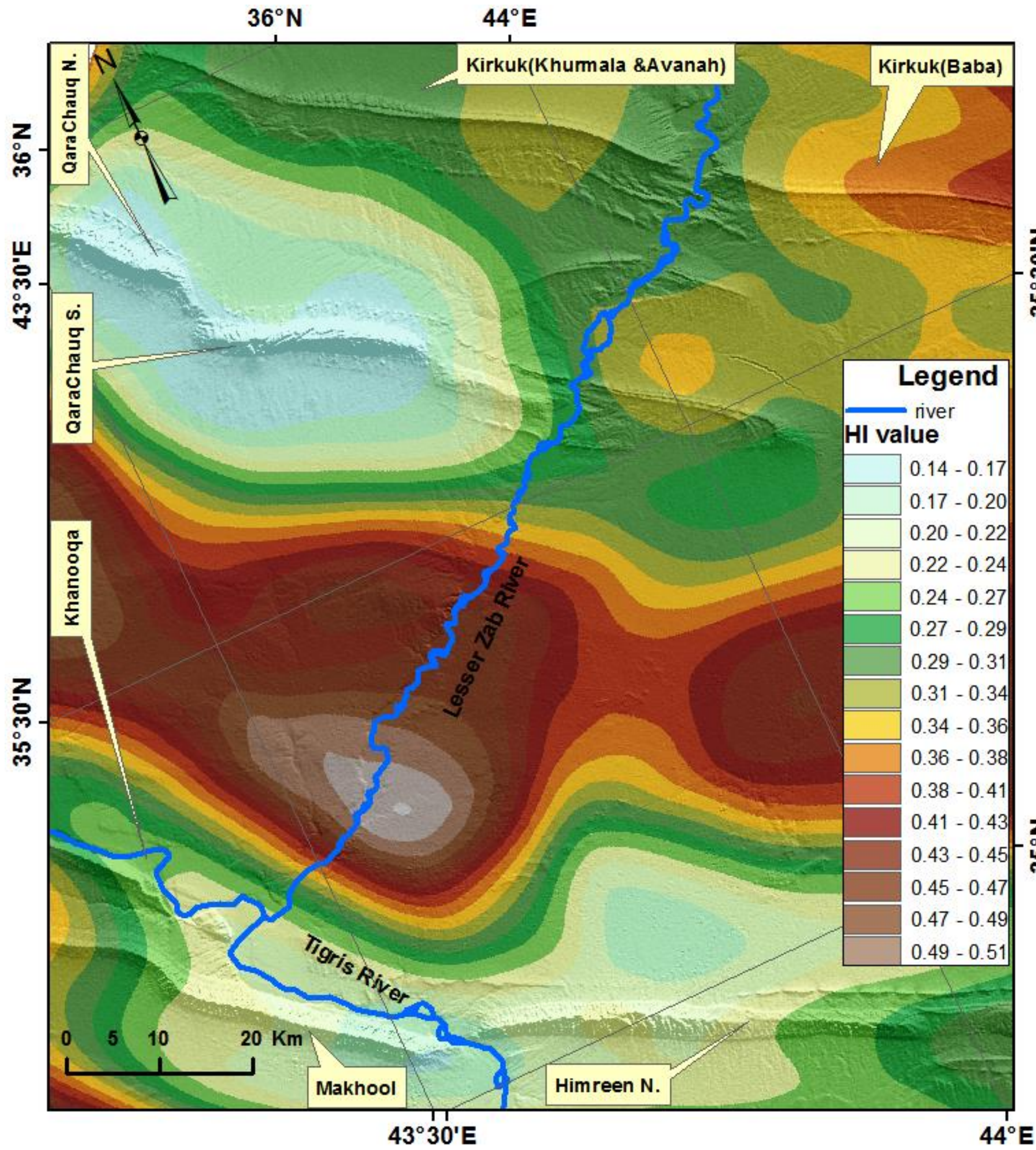

Fig. 5. Hypsometric Integral (HI) map for the study area in the Kirkuk Embayment.

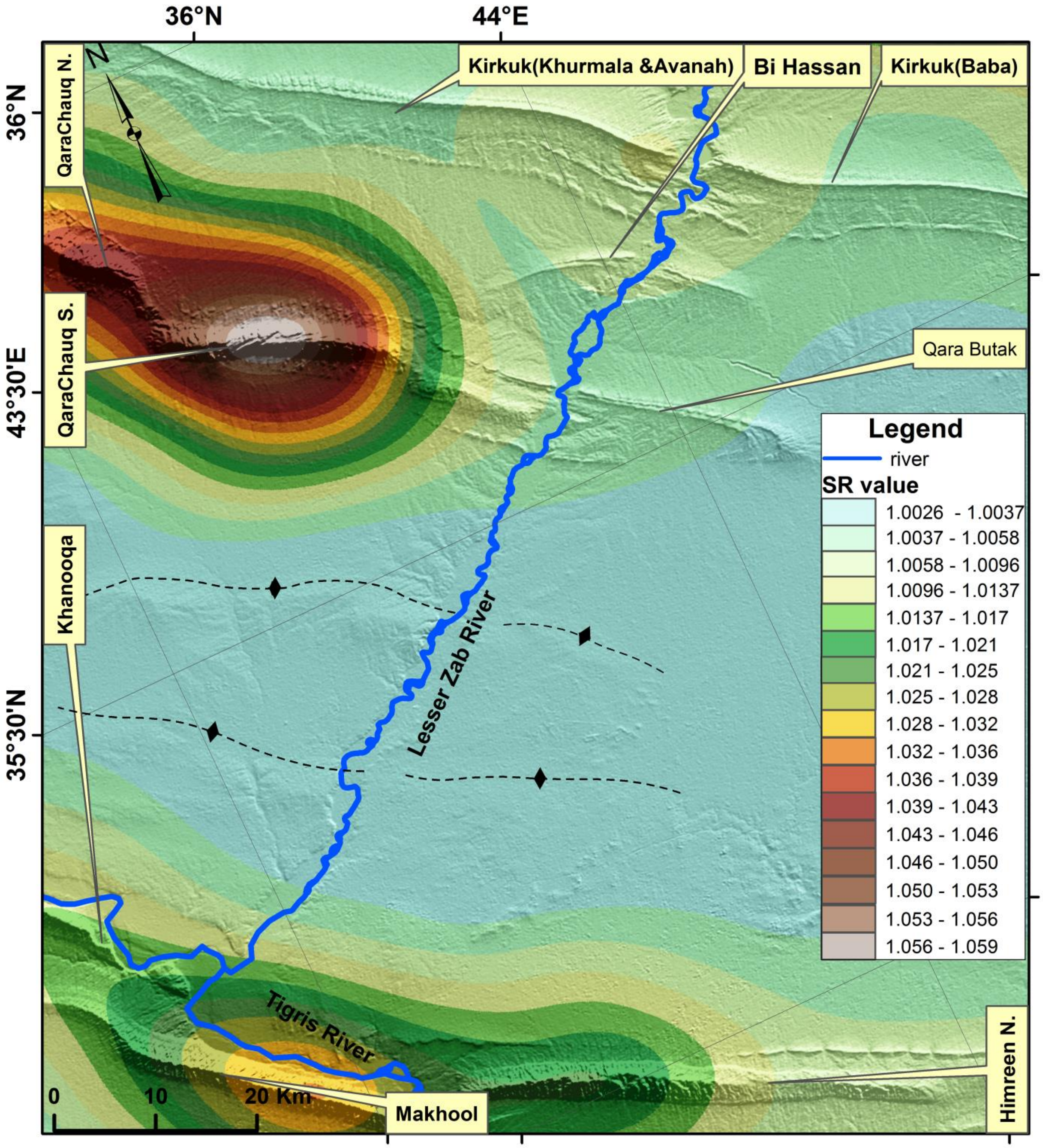

Fig. 6. Surface Roughness (SR) map, showing different degree of dissection.

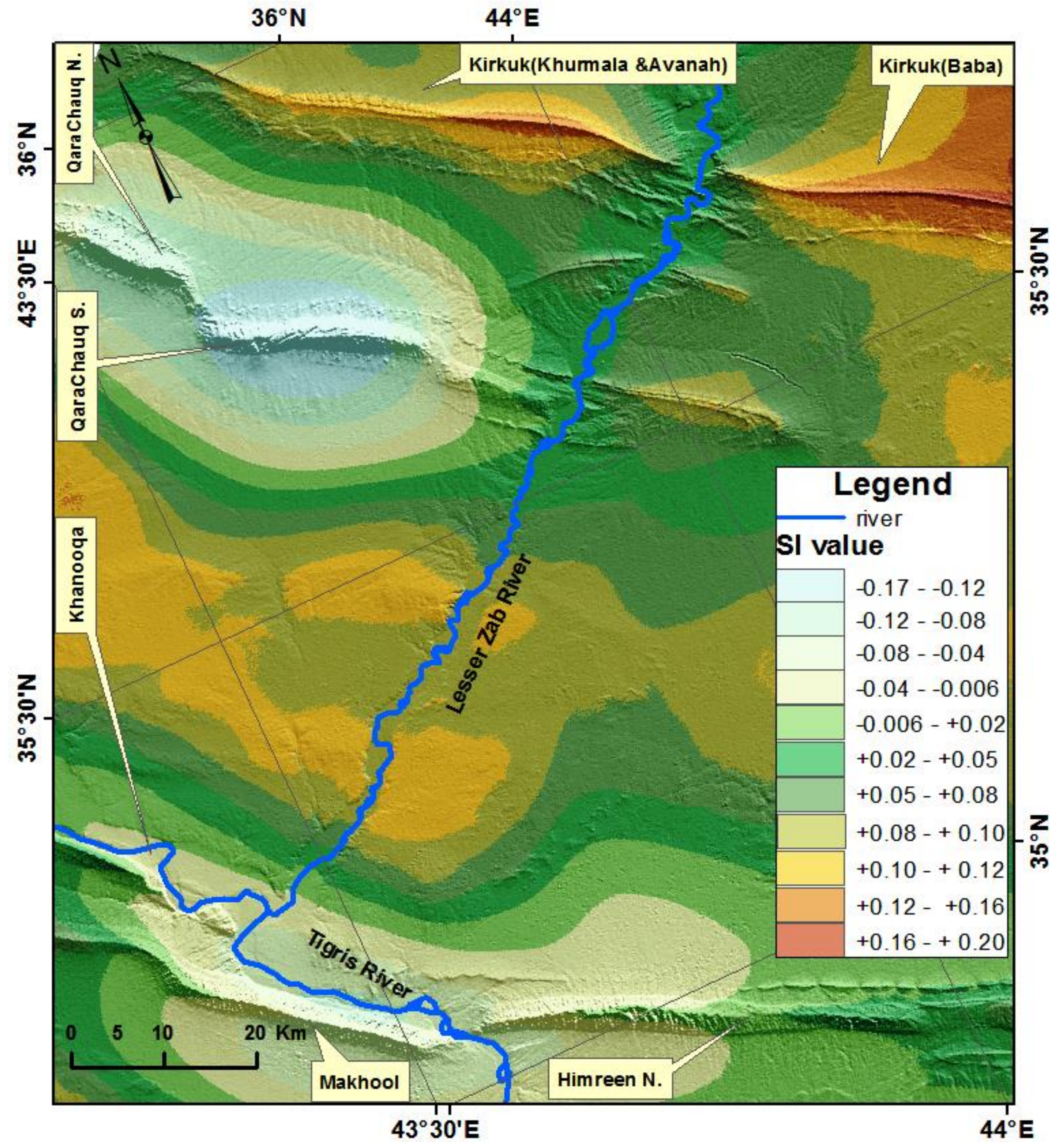

Fig. 7. Surface Index (SI) map showing different stage of landscape maturity in the Kirkuk Embayment. The positive values represent relatively less mature areas and the negative values represent relatively more mature areas. See text for details.

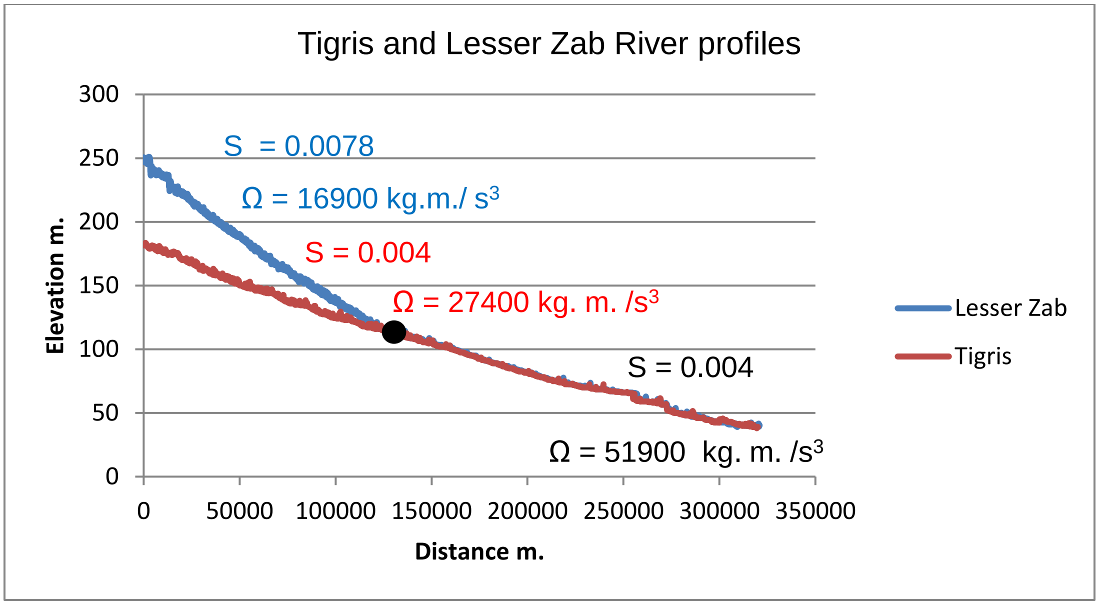

Fig. 8. Longitudinal profile of the Lesser Zab River and Tigris River showing the gradient (S) and stream power (Ω) of the two rivers. Also there is no change in the base level of the river as knickpoints. The solid black circle represents the confluence point between Lesser Zab River and Tigris River.

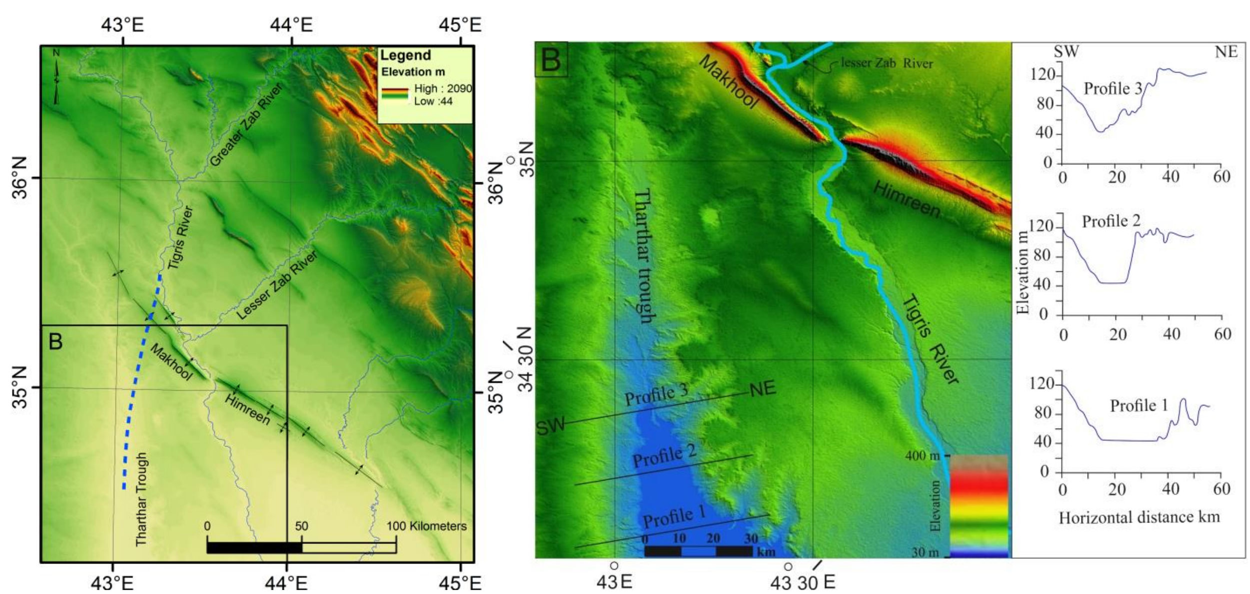

Fig. 9. Map showing the location of the Tharthar trough, and the possibility for it being a palaeo-channel of Tigris River (inset B). The dashed blue line is the plausible pathway for the Tigris River.

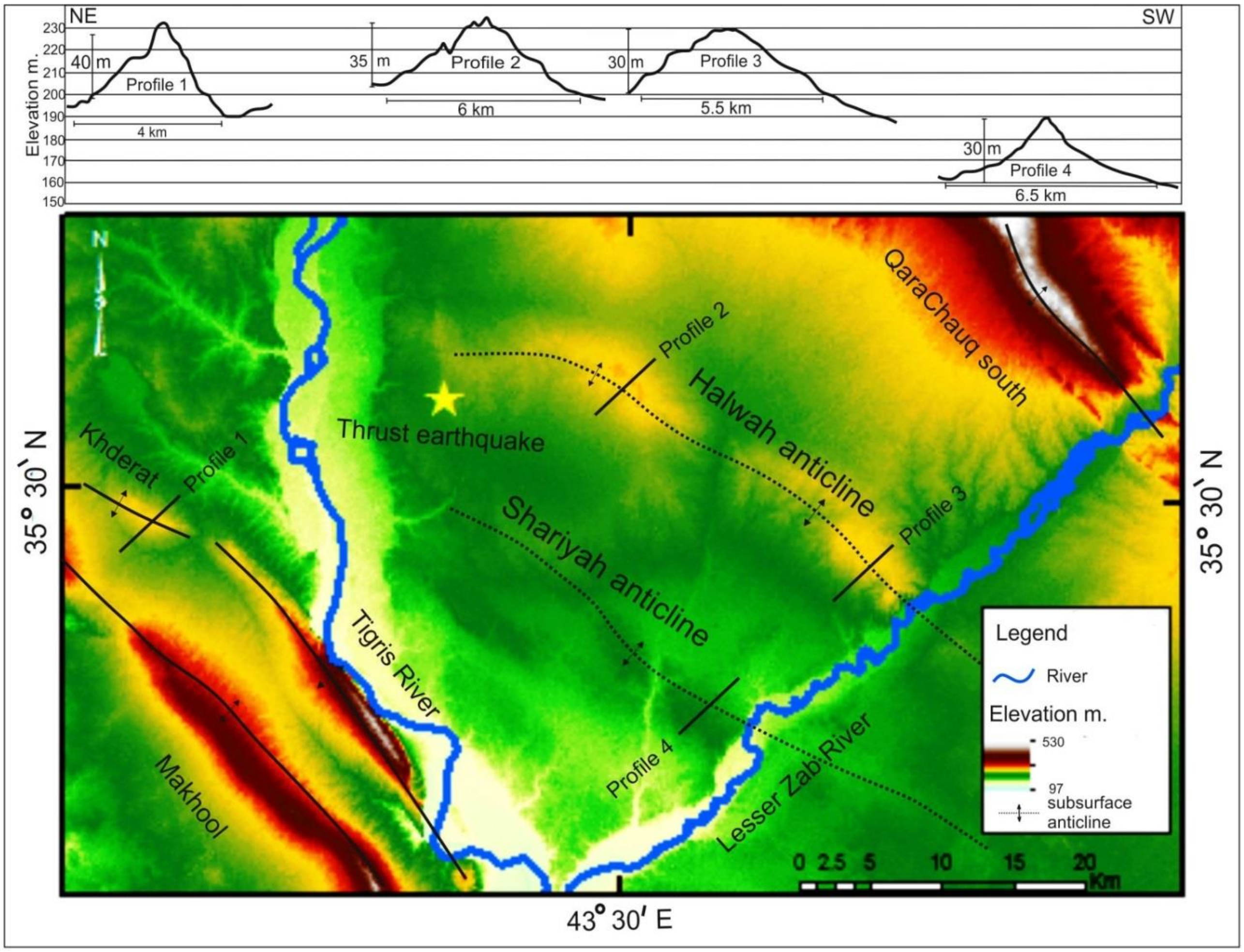

Fig. 10. Topographic analysis of SRTM data, showing the subdued expressions of the new anticlines between QaraChauq and Makhool/ Himreen.

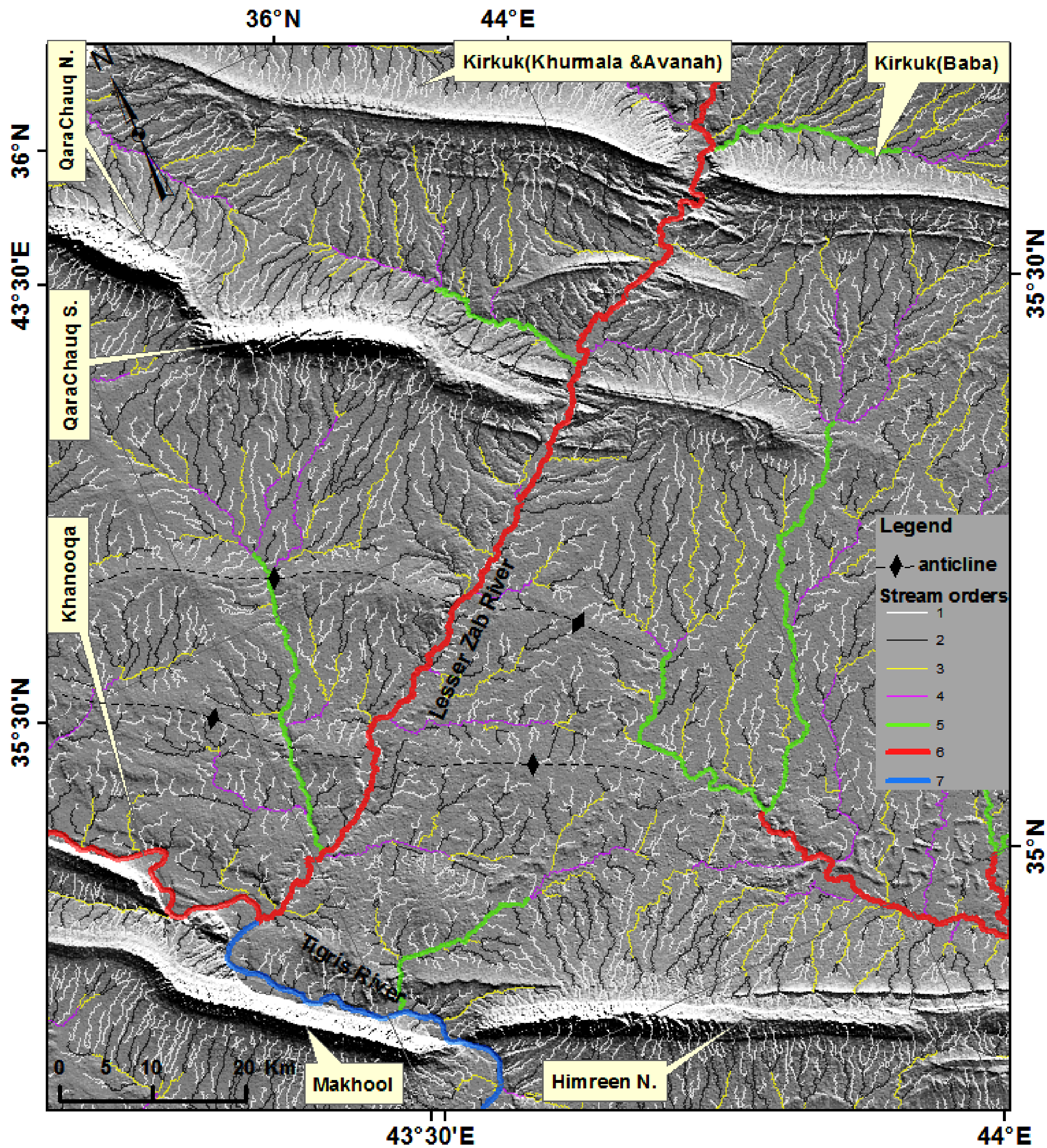

Fig. 11. Drainage network of the Kirkuk-Himreen area extracted from SRTM 90m according to the hierarchical order of Strahler using TecDEM software. Note the radial pattern that reflects the subsurface uplift around the new anticlines.

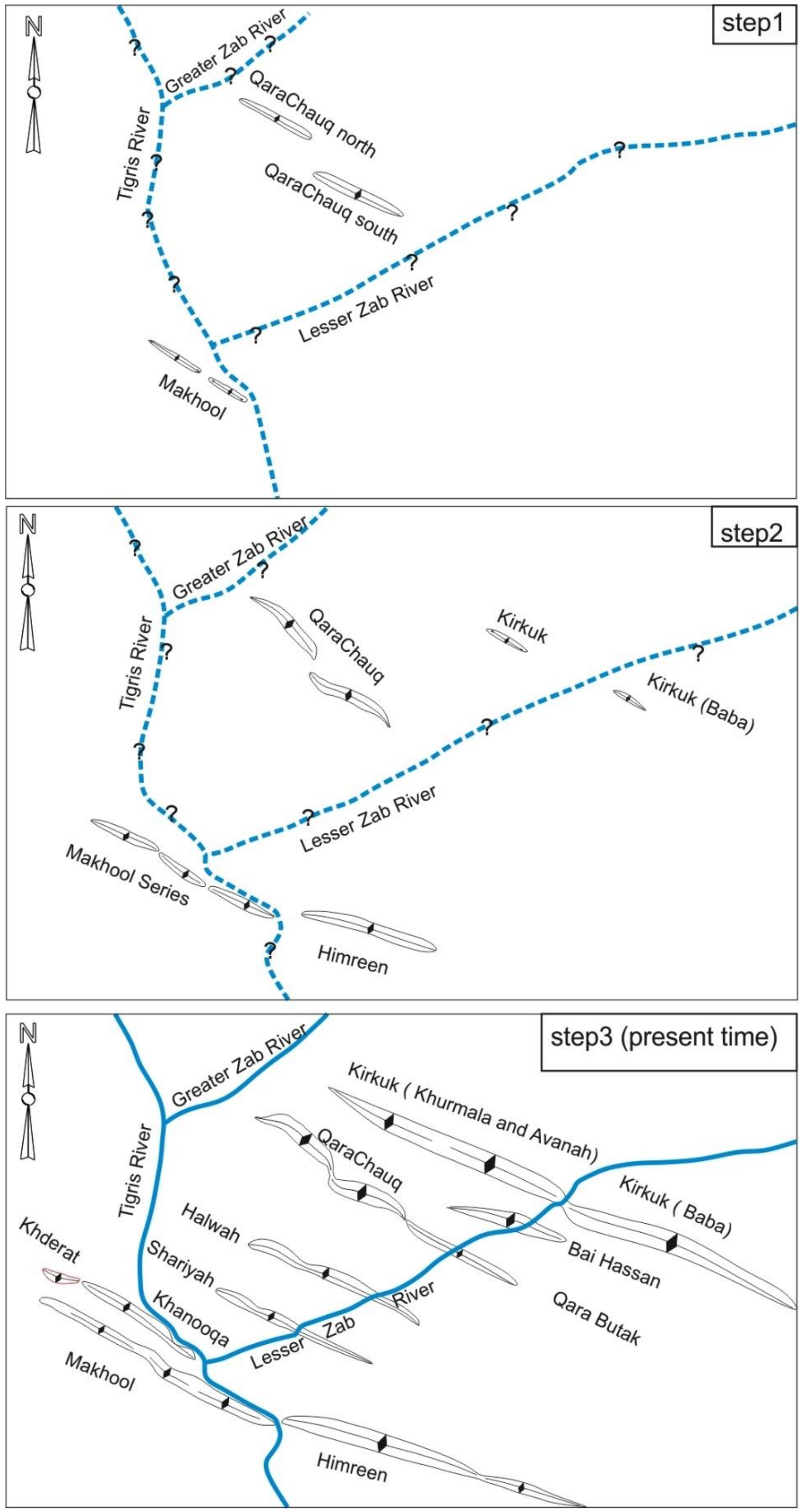

Fig. 12. Conceptual model of anticline growth in the Kirkuk Embayment.

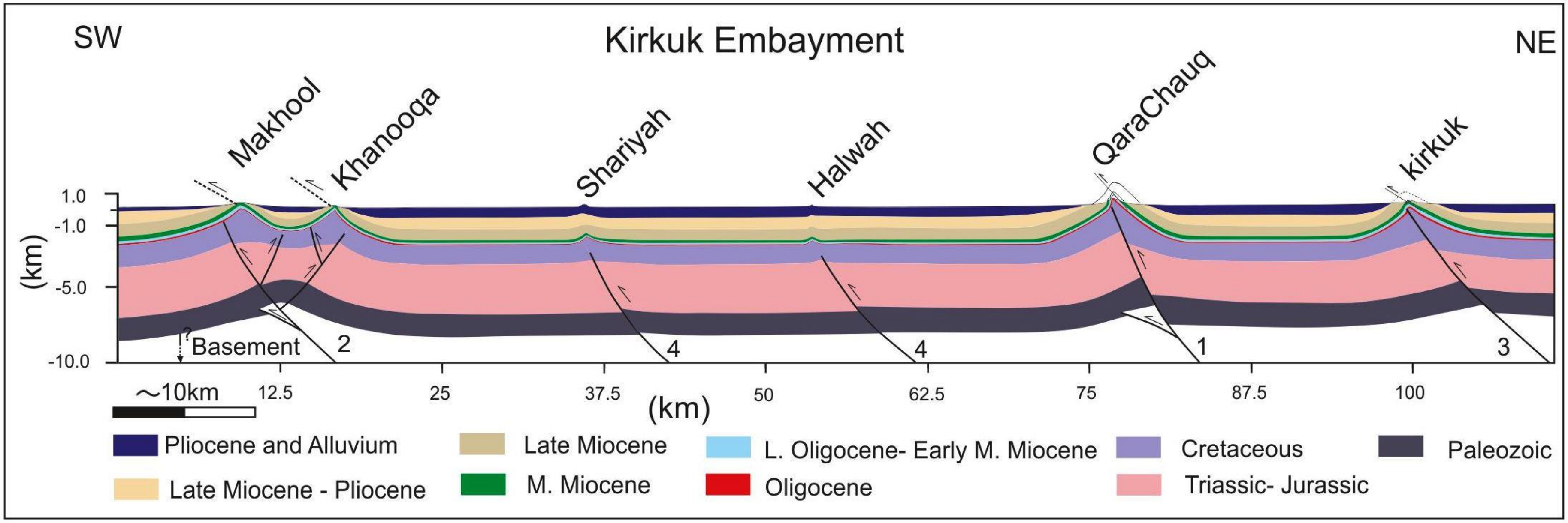

Fig. 13. Balanced cross-section of the Kirkuk Embayment developed using landscape maturity, unpublished surface data (Othman et al. 2004) and published subsurface data (Kent 2010), earthquake data (Fig. 2), and field observations from the eastern margin of the Kirkuk Embayment. This model shows the local detachment in the Fat'ha Formation and the involvement of basement faults in the deformation. Numbers refer to order of faulting: see text.